약학석사학위논문

PPARγ-dependent obesogenic activity of benzophenone sunscreens

벤조페논 계열 자외선차단제의 PPARγ 기전을 통한 비만유도 활성 연구

2021 년 2 월

서울대학교 대학원
약학과 천연물과학전공

Jeayoung Christina Shin

PPARγ-dependent obesogenic activity of benzophenone sunscreens

벤조페논 계열 자외선차단제의
PPARγ 기전을 통한 비만유도 활성 연구

지도교수 노 민 수

이 논문을 약학석사 학위논문으로 제출함
2021년 2월

서울대학교 대학원
약학과 천연물과학전공
신 지 영

신지영의 석사학위논문을 인준함
2020년 12월

위 원 장 이 상 국 (인)

부위원장 박 성 혁 (인)

위 원 노 민 수 (인)

Abstract

PPARγ-dependent obesogenic activity of benzophenone sunscreens

Jeayoung C. Shin

Department of Pharmacy

The Graduate School

Seoul National University

Obesogens are exogenous chemicals that can promote adipogenesis in adipose or non-adipose tissues. Recently, the obesogenic activity of avobenzone, a long wave ultraviolet (UV) A filter, was elucidated in the adipogenesis model of human bone marrow mesenchymal stem cells (hBM-MSCs). Among the approved sunscreen filters, benzophenone-3 (BP-3) and benzophenone-8 (BP-8) showed high similarity values to avobenzone. BP-3 and BP-8 are commonly used UV filter ingredients in diverse sunscreen products. In this study, the obesogenic potentials of BP-3 and BP-8 were investigated due to their chemical similarity to avobenzone. During the adipogenesis in hBM-MSCs, BP-3 and BP-8 (EC_{50}, 25.05 and 43.20 μM, respectively) potently promoted adiponectin secretion than avobenzone (EC_{50}, 72.69 μM). In target identification studies, both BP-3 and BP-8 directly bound to peroxisome proliferator-activated receptor γ (PPARγ), which was associated with the recruitment of steroid receptor coactivator-2 (SRC-2). BP-3 functioned as a PPARγ full agonist whereas BP-8 was a PPARγ

partial agonist. In addition, BP-3 and BP-8 significantly increased the gene transcription of PPARα, PPARγ, and major lipid metabolism-associated enzymes in human epidermal keratinocytes, a major target site of UV filters in human skin. This study suggests that BP-3 and BP-8 are obesogenic environmental chemicals similar to phthalates, bisphenols, and organotins.

Keywords: Benzophenone-3, Benzophenone-8, PPARγ, Human bone marrow mesenchymal stem cells, Obesogenic

Student number: 2018-21004

Table of Contents

List of Figures

1. Introduction

Benzophenone-3 (BP-3; oxybenzone) and benzophenone-8 (BP-8; dioxybenzone) are extensively used as organic sunscreen ingredients for broad spectrum ultraviolet (UV) absorption (Calafat et al., 2008; Mao et al., 2018). BP-3 is approved in many countries as an active ingredient in sunscreen. The regulations of the US Food and Drug Administration (FDA) allow the use of BP-3 and BP-8 at concentrations of up to 6% and 3%, respectively, in over-the-counter sunscreen products (Wang and Lim, 2011). In cosmetic regulation by the European Union (EU), BP-3 is approved at a concentration of 10% in cosmetic products (Jansen et al., 2013).

To provide better protection against UV light, some countries have permitted the combined use of several benzophenone (BP) derivatives in sunscreen formulations (Mao et al., 2018). Despite the health benefits of organic sunscreen ingredients such as anti-skin aging and prevention of cutaneous tumorigenesis, adverse health effects of BP-3 and BP-8 have also been reported, including contact allergy and phototoxicity (Collins and Ferguson, 1994; Heurung et al., 2014). Notably, BPs have been suspected to have endocrine disrupting potential because they exhibited slight estrogenic activity in both in vitro and in vivo studies (Ghazipura et al., 2017; Lee et al., 2018b).

Recently, we reported that avobenzone, a long wave UVA filter in sunscreen products, exhibits obesogenic activities in human epidermal keratinocytes and human bone marrow mesenchymal stem cells (hBM-MSCs) (Ahn et al., 2019). During adipogenesis in hBM-MSCs, avobenzone significantly promoted both lipid accumulation and adiponectin production similar to reference obesogens, such as bisphenol A, butylparaben, benzyl butyl phthalate, and tributyltin. Although avobenzone did not directly bind to PPARγ, it affected the functions of PPARγ in both human keratinocytes and mesenchymal stem cells (Ahn et al., 2019). Although

sunscreen products are indispensable to protect human skin from photoaging and the risk of melanoma development, their environmental exposure has raised concerns regarding human health. Currently, it is not known whether UV filters in sunscreen products have obesogenic potential.

Obesogens are exogenous chemicals that can promote adipogenesis in adipose or non-adipose tissues (Heindel and Blumberg, 2019). Environmental obesogens such as phthalates, bisphenols, and organotins are extensively used in plastics, thermal paper, pesticides, and marine antifoulants, and may contribute to the obesity pandemic in humans. The molecular and cellular targets of these environmental obesogens are associated with nuclear hormone receptors such as estrogen receprors (ER), glucocorticoid receptors (GR) and peroxisome proliferator-activated receptors (PPAR) (Heindel and Blumberg, 2019). Tributyltin (TBT), a major organotin chemical used in marine antifoulants or fungicides in industrial water systems, directly binds to PPARγ, a major nuclear receptor that regulates cellular metabolic processes.

Chemical toxicity can be predicted based on chemical similarity (McKinney et al., 2000). Avobenzone has aromatic ketone and methoxyphenyl moieties, which have common chemical structures to those in BP sunscreens. Although BP-3 and BP-8 are chemically similar to avobenzone, these sunscreen constituents have not yet been investigated as potential metabolic obesogens. Therefore, in this study, the obesogenic potential of BP-3 and BP-8 was investigated using the adipogenesis model of hBM-MSCs.

2. Materials and Methods

2-1. Chemical similarity analysis

The chemical structures of BP-3, BP-8, avobenzone (AVB), benzyl butyl phthalate (BBP), and bis(2-ethylhexyl) phthalate (DEHP), are represented in the SMILES format. For example, BP-3 is described as “COC1=CC(=C(C=C1)C(=O)C2=CC=CC=C2)O". SMILES formatted structures were converted into the binary PubChem fingerprints using the *get.fingerprint* function from “rcdk” package in R (R Core Team). The 881-length binary fingerprints were described by a combination of 0 (indicating an absence of a certain structural feature) and 1 (indicating a presence of a certain structural feature). Each bit in the 881-length chemical fingerprint was compared to calculate chemical similarity. To determine the structural similarity between sunscreen ingredients, the chemical fingerprint-based Jaccard index was calculated. The Jaccard index is defined as the intersection between the chemical fingerprint sets of two compounds over the union between the sets (Luechtefeld et al., 2018). Accordingly, the Jaccard index is a numerical measure of similarity ranging from zero to one (identical structure). A pair of compounds with similar structures has a higher Jaccard index.

2-2. Cell culture and differentiation of hBM-MSCs

The hBM-MSCs were purchased from Lonza (Walkersville, MD, USA) and were cultured in Dulbecco’s Modified Eagle Medium (DMEM) with low glucose (1 g/L) supplemented with 10% fetal bovine serum (FBS), 1% penicillin-streptomycin, and 1% Glutamax™ (Invitrogen, Carlsbad, CA, USA). To induce adipocyte differentiation, the culture medium was replaced with DMEM containing high-glucose (4.5 g/L) supplemented with 10% FBS, 1% penicillin-streptomycin, 10 μg/mL insulin, 0.5 μM dexamethasone, and 0.5 mM isobutylmethyxanthine (IBMX). Insulin, dexamethasone, IBMX, and pioglitazone (PIO) were purchased from Sigma-

Aldrich Chemical Company (St. Louis, MO, USA).

2-3. Oil Red O staining and quantification

Oil Red O (ORO) staining was performed to assess lipid accumulation in differentiated adipocytes (Han et al., 2018). Cells were washed twice with phosphate-buffered saline (PBS), fixed with 10% formalin in PBS for 1 h, washed with 60% isopropanol, and then allowed to dry completely. Lipid droplets in the cells were stained with 0.2% ORO reagent for 20 min at room temperature, and then, the cells were washed with tap water three times. To quantify the lipid accumulation, ORO stained hBM-MSCs were dissolved with 100% isopropanol for 10 min at room temperature and the absorbance was measured at 540 nm using a spectrophotometer (Ahn et al., 2019). To visualize the nuclei, hBM-MSCs were counterstained with hematoxylin reagent for 2 min and then washed three times with tap water. The level of adipocyte differentiation was observed and photographed using an Eclipse TS100 inverted microscope (Nikon Co., Tokyo, Japan).

2-4. Quantitative real-time reverse transcription polymerase chain reaction

Quantitative real-time reverse transcription polymerase chain reaction (Q-RT-PCR) was performed to quantify the expression levels of target mRNAs using an AB7500 System (Applied Biosystems, Foster City, CA, USA). The TaqMan expression primer sets used in the Q-RT-PCR were: peroxisome proliferator activated receptor alpha (PPARα), Hs00231882_m1; PPARγ, Hs00234592_m1; 3-hydroxy-3-methylglutaryl-CoA reductase (HMGCR), Hs00168352_m1; 3-hydroxy-3-methylglutaryl-CoA synthase 1 (HMGCS1), Hs00940429_m1; fatty acid binding protein 4 (FABP4), Hs00609791_m1; and adiponectin (ADIPOQ), Hs00605917_m1. Human glyceraldehyde 3-phosphate dehydrogenase (GAPDH), Hs02786624_g1 was used as a control gene. Quantification of relative expression levels was performed using a mathematical model developed by Pfaffl (2001).

2-5. Time-resolved fluorescence resonance energy transfer based PPAR binding and coactivator assays

The time-resolved fluorescence resonance energy transfer (TR-FRET)-based receptor binding assay was performed using Lanthascreen^{TM} competitive binding assay kits (Invitrogen) to evaluate the ligand binding to PPARα, PPARγ, and PPARδ. Lanthascreen^{TM} coactivator assay kits were used to determine the effects of ligands on the receptor coregulation of PPARγ. Fluorescein-labeled coactivator peptides SRC-2 (sequence KKKENALLRYLLDKDDTKD), RAP250 (sequence VTLTSPLLVNLLQSDISAG), DRIP-1 (sequence KVSQNPILTSLLQITGNGG), RIP140 (sequence SHQKVTLLQLLLGHKNEEN), and PGC-1α (sequence EAEEPSLLKKLLLAPANTQ) were used. Assay plates were read at wavelengths of 520 nm and 495 nm after 1 h to 2 h incubation, using CLARIOstar (BMG LABTECH, Ortenberg, Germany). All instrument settings were according to the TR-FRET manufacturer's instructions. GW7647, GW1929, and GW501516 were purchased from Tocris Bioscience (Bristol, U.K.).

2-6. Computational docking analysis

Computational docking studies of compounds were performed using the AutoDock Vina 1.1.2 (Scripps Research Institute, La Jolla, CA, USA) (Trott and Olson, 2010). PPARγ-LBD structure for the docking analysis was obtained from Research Collaboratory for Structural Bioinformatics (RCSB) Protein Database (PDB: 5Y2O) (Lee et al., 2017). The docking site of ligands to PPARγ-LBD was defined as a 30 Å^3 grid box with the centroid of the originally co-crystalized ligand, pioglitazone. The energy-minimized ligand-binding pose of each compound was selected to compare closely contacting residues in the binding pocket. The protein-ligand interaction analysis was performed using LigPlot+ 1.4.5 (Wallace et al., 1995). All the graphics displaying the computational docking results were visualized using PyMOL (Schrödinger, LCC,

New York, NY, USA).

2-7. Statistical analysis

Statistical analysis was conducted using the statistical package for the social sciences (SPSS®) for Windows (SPSS Science, Chicago, IL, USA). Student's *t*-test was used to compare single-treated groups and the experimental control. A one-way analysis of variance (ANOVA), followed by Tukey's *post hoc* tests for multiple comparison were also performed.

3. Results

3-1. BP-3 and BP-8 are potential metabolic obesogens

BP-3 and BP-8 have chemical structures in common with the aromatic ketone and methoxyphenyl moieties of avobenzone, a compound promoting adipogenesis in hBM-MSCs (Fig. 1A). To determine the chemical similarity of BP-3 and BP-8 to the obesogens AVB, BBP, and DEHP, PubChem chemical fingerprints were derived for each compound and the Jaccard similarity was calculated (Fig. 1B). The Jaccard index is defined as the ratio of the number of common structural features to the total number of structural features when two given compounds are expressed as chemical fingerprints. Thus, the Jaccard index is proportional to the structural similarity between two compared chemicals. The Jaccard index between avobenzone and BPs was 0.80, which represented a higher similarity value than those of BBP and DEHP (Fig. 1B). The chemical similarity between avobenzone and BPs suggests that BP-3 and BP-8 may have similar chemical properties.

Consequently, the effects of BP-3 and BP-8 on adipogenesis in hBM-MSCs were evaluated to determine whether BPs are potential obesogens similar to avobenzone. To evaluate the obesogenic properties of BP-3, BP-8, and other positive chemical obesogens using hBM-MSCs, the compounds were added to the adipogenic chemical cocktail consisting of insulin, dexamethasone, and isobutylmethylxanthine (IDX condition). For the preliminary screening for the effects of test chemicals on adipogenesis, a 30 μM concentration was chosen to compare with the effect of avobenzone except TBT (Ahn et al., 2019). As TBT exhibited significant cytotoxicity to hBM-MSCs up to 1 μM, non-cytotoxic concentration (0.1 μM) was treated with IDX. The adipogenesis-promoting activity was measured using ORO staining on day 5 after induction of adipogenesis in hBM-MSCs (Fig. 2A). During adipogenesis of hBM-MSCs, BP-3 and BP-8 significantly increased the size and numbers of lipid droplets in differentiated

adipocytes similar to the other reference obesogens, BBP, DEHP, and tributyltin (TBT) (Fig. 2A). Quantification of ORO staining showed that PIO (1 μM) and TBT (0.1 μM) increased adipogenesis by 3.61 and 3.85-fold, respectively. When adipogenesis promoting activities were compared at 30 μM, BP-3, BP-8, AVB, BBP, and DEHP increased the stained ORO levels by 2.10, 2.22, 1.91, 2.84, and 1.42-fold, respectively (Fig. 2B). Therefore, BP-3 and BP-8, which have higher chemical similarity values to the chemical fingerprint of avobenzone than that of the other compounds promoted adipogenesis in hBM-MSCs, suggesting their obesogenic potential.

To confirm the obesogenic potential of BP-3 and BP-8 during adipogenesis in hBM-MSCs, the changes they induced in adipogenic biomarkers were compared with those induced by avobenzone (Ahn et al., 2019). Similar to avobenzone, both BP-3 and BP-8 significantly upregulated the gene transcription of quantitative biomarkers for mammalian adipogenesis, adiponectin and FABP4, during adipogenesis of hBM-MSCs compared to the IDX control (Fig. 3A and B). In addition, BP-3 and BP-8 significantly increased the mRNA levels of PPARγ, a master nuclear hormone receptor regulating mammalian adipogenesis (Fig. 3D). Next, the protein levels of adiponectin promoted by BPs or representative obesogens were compared in cell culture supernatants during adipogenesis in hBM-MSCs (Fig. 4A). BP-3, BP-8, AVB, BBP, DEHP, TBT, and PIO increased adiponectin secretion by 3.20, 3.23, 2.60, 4.50, 1.75, 3.60, and 6-fold, respectively, compared to the IDX control (Fig. 4A). When the maximum response achieved by pioglitazone, a PPARγ agonist, was used as 100% reference, half-maximal effective concentration (EC_{50}) values of BP-3, BP-8, AVB, PIO, and TBT were 25.05, 43.20, 72.69, 0.44, and 0.080 μM, respectively (Fig. 4B). Therefore, BP-3 and BP-8 promoted adiponectin production during adipogenesis of hBM-MSCs in a concentration-dependent manner.

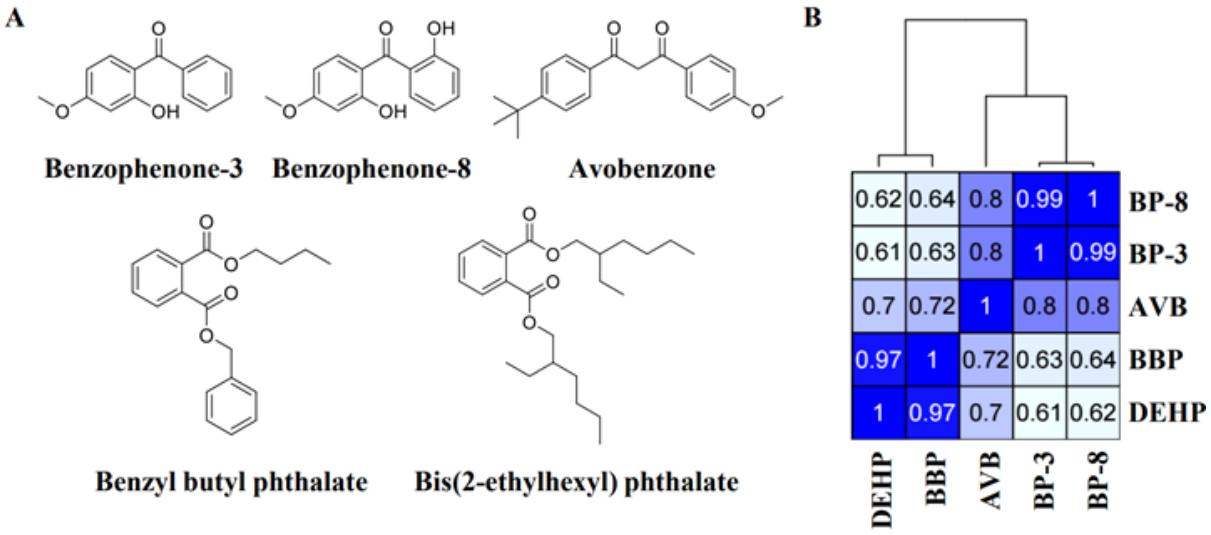

Figure 1. Investigation of BP-3 and BP-8 as potential metabolic disrupting obesogens

(A) Chemical structures of BP-3, BP-8, AVB, BBP, and DEHP. (B) Structural similarities between obesogenic compounds were calculated using Jaccard index.

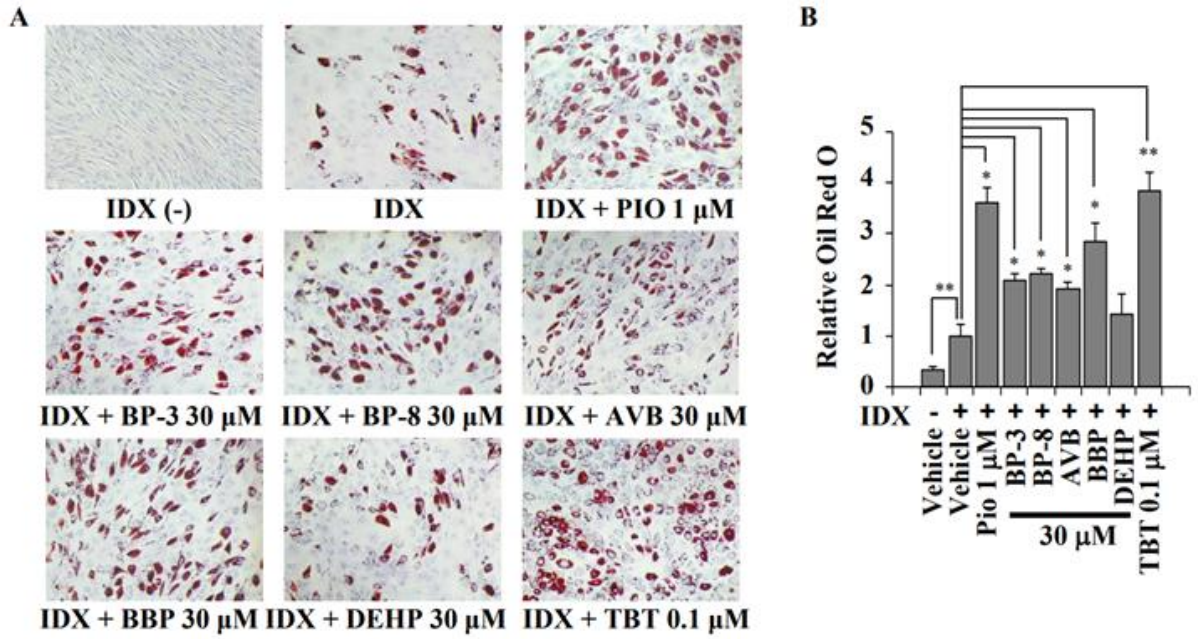

Figure 2. Evaluation of adiponectin secretion-promoting activity of BP-3 and BP-8 in hBM-MSCs

BP-3, BP-8, or other positive chemical obesogens were added to IDX medium when adipogenesis was induced in hBM-MSCs. Adipogenic medium containing obesogenic compounds was exchanged twice during 6-day differentiation process. On day 6, (A) Oil Red O (ORO) staining was performed to visualize lipid droplets formed during adipogenesis of hBM-MSCs. (B) ORO levels were then quantified by measuring absorbance at 540 nm. Values represent the mean expression level ± SD (n=3), *$p < 0.05$; **$p < 0.01$.

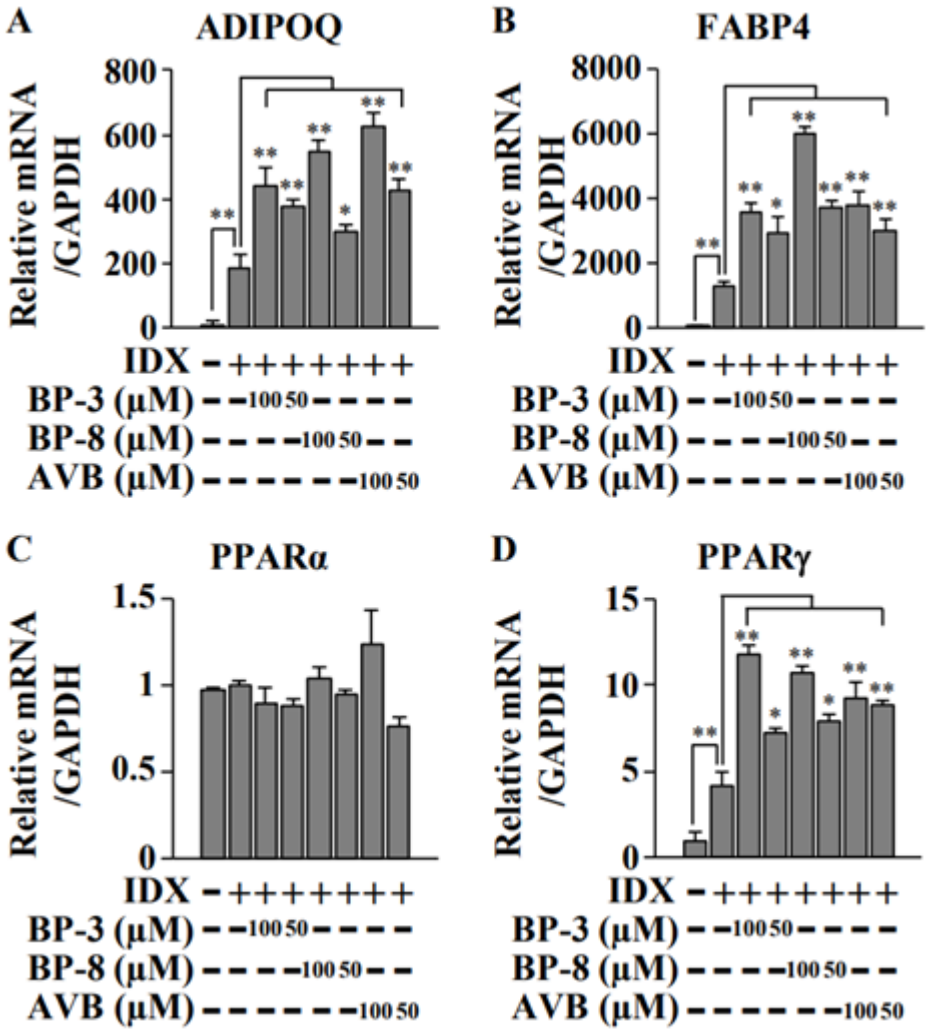

Figure 3. The effect of BP-3 and BP-8 on adipogenic biomarker expression during adipogenesis in hBM-MSCs

BP-3, BP-8, and other positive chemical obesogens were added to IDX medium when adipogenesis was induced. To determine mRNA levels in BP-3-, BP-8-, and avobenzone-treated hBM-MSCs, total RNA samples were extracted on day 5 of differentiation process. mRNA levels of ADIPOQ (A), FABP4 (B), PPARα (C) and PPARγ (D) were measured by Q-RT-PCR. Values represent the mean expression level ± SD (n=3), *$p < 0.05$; **$p < 0.01$.

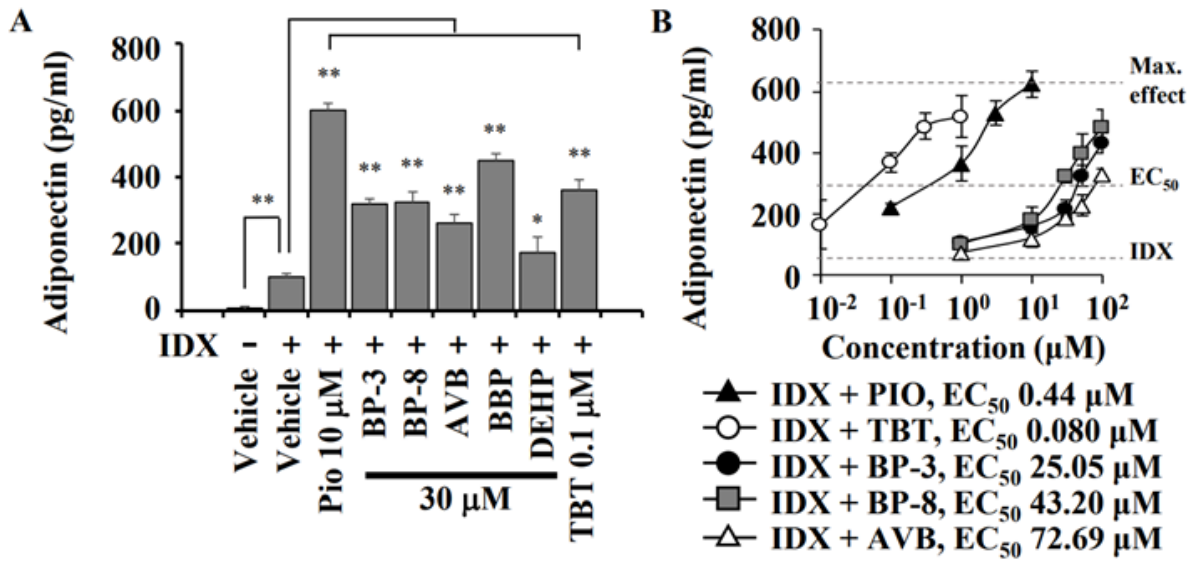

Figure 4. The effects of adiponectin secretion-promoting activity in hBM-MSCs

(A) Adiponectin concentrations were measured after treatment with BP-3, BP-8, AVB, BBP, DEHP, TBT, and PIO. (B) Concentration dependency of BP-3, BP-8, AVB, TBT, and PIO on adiponectin-secretion-promoting activity was determined. Values represent the mean expression level ± SD (n=3), *$p < 0.05$; **$p < 0.01$.

3-2. BP-3 and BP-8 directly bind to PPARγ

Peroxisome proliferator-activated receptors, PPARα, PPARγ, and PPARδ, regulate adipogenesis and major metabolic processes, which are mainly affected by obesogens (Ma et al., 2018). To investigate whether the adipogenesis-promoting activity of BP-3 and BP-8 in hBM-MSCs was associated with the cellular PPAR pathway, TR-FRET-based competitive PPAR binding assays were performed using AVB, BBP, and DEHP as positive obesogenic controls (Fig. 5). BP-3, BP-8, and BBP exhibited competitive binding activity to PPARγ but they did not affect the labeled ligand binding to either PPARα or PPARδ (Fig. 5). At 50 μM, BP-3, BP-8, and BBP significantly inhibited the labeled PPARγ ligand binding activity by 50.1, 65.9, and 65.2%, respectively (Fig. 5C). TBT, a potent PPARγ binding obesogen (Ahn et al., 2019), was also included as a positive control and 0.1 μM significantly replaced the PPARγ binding activity by 79.6%. As previously reported, avobenzone and DEHP replaced less than 50% of the PPARγ binding activity (Fig. 5C). In concentration-effect analyses, the *Ki* values of BP-3 and BP-8 were calculated as 26.23 and 16.54 μM, respectively (Fig. 5D). These results support the notion that the adipogenesis-promoting activity of BP-3 and BP-8 is mediated via the PPARγ pathway.

To investigate whether BP-3 and BP-8 induce PPARγ transactivation, a TR-FRET PPARγ coactivator assay was performed (Fig. 6). Because PPARγ interacts with diverse coactivator proteins to regulate gene transcription (Viswakarma et al., 2010), the major PPARγ coactivators, SRC-2, RAP250, DRIP-1, RIP140, and PGC-1α, were tested (Fig. 6A). Determination of BP-3- or BP-8-induced recruitment of coactivator peptides, corresponding to SRC-2, RAP250, DRIP-1, RIP140, and PGC-1α, showed a significant increase in coactivator peptide SRC-2 recruitment to the PPARγ ligand-binding domain (LBD) (Fig. 6A). In a concentration-effect analysis, the EC_{50} value of BP-8 was 73.39 μM. Although BP-3 exhibited concentration-

dependent effects, it was less potent than BP-8 was. Therefore, both BP-3 and BP-8 directly regulate PPARγ functions through a SRC-2 coactivator-dependent mechanism.

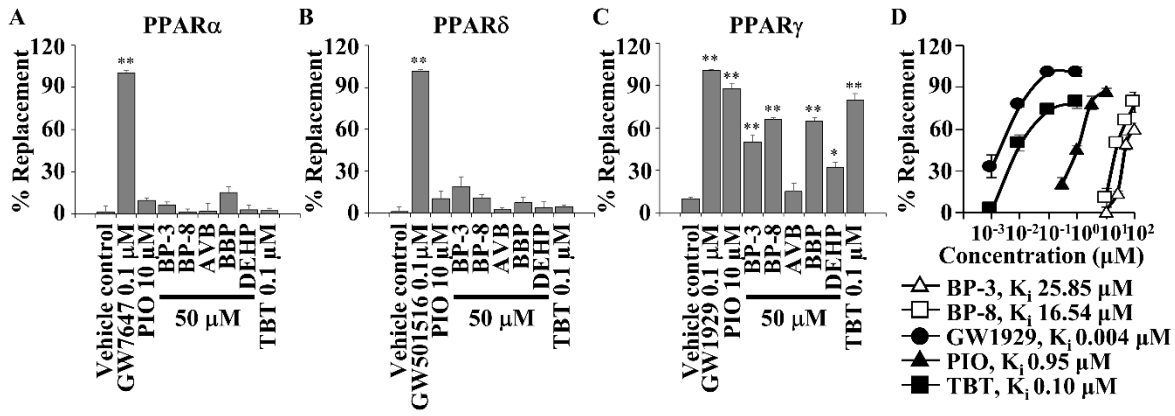

Figure 5. Target identification of adipogenesis-promoting activity of BP-3 and BP-8

TR-FRET competitive binding assays of PPARα (A), PPARδ (B), and PPARγ (C) were performed with BP-3, BP-8, AVB, BBP, DEHP, and TBT. (D) Based on Cheng and Prusoff equation, *Ki* values were calculated for PPARγ binding activity of obesogenic compounds. Positive controls were GW1929 and pioglitazone (PIO). Values represent the mean expression level ± SD (n=3), *$p < 0.05$; **$p < 0.01$.

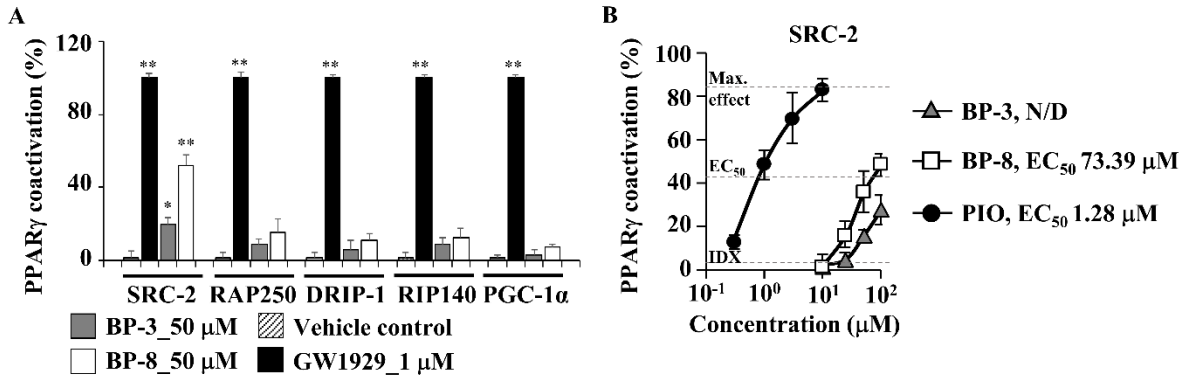

Figure 6. Functional outcomes of BP-3 and BP-8 on PPARγ binding

(A) TR-FRET PPARγ coactivator recruitment assay was performed with coactivator peptide SRC-2, RAP250, DRIP-1, RIP140, and PGC-1α, labeled with fluorescein. BP-3, BP-8, and PPARγ agonist GW1929 were tested. (B) Concentration-dependent effect of obesogenic compounds on peptide SRC-2 was determined. Positive control was pioglitazone (PIO). Values represent the mean expression level ± SD (n=3), *$p < 0.05$; **$p < 0.01$.

3-3. BP-3 and BP-8 have different binding modes of PPARγ ligand binding domain

To understand the structural basis of BP-3- and BP-8-induced PPARγ transactivation, molecular docking simulation was performed using a three-dimensional model constructed with the X-ray crystal structure of a PPARγ-LBD-pioglitazone complex (PDB ID: 5Y2O; Lee et al., 2017) (Fig. 7A). In the energy-minimized docking model, BP-3 was located in the hydrophilic binding pocket of the PPARγ-LBD near helix (H) 12 (Fig. 7B). In contrast, BP-8 interacted with amino acid residues in the hydrophobic binding pocket between H3 and β-sheets (Fig. 7C). The binding free energies of BP-3 and BP-8 were -6.7 and -6.3 kcal/mol, respectively. BP-3 interacted with amino acid residues Cys285 (H3), Gln286 (H3), Arg288 (H3), Ser289 (H3), and Tyr473 (H12).

In addition, the 2-hydroxyl group of the 4-methoxyphenyl and ketone moieties of BP-3 formed a hydrogen bond between the phenolic hydroxyl group of Tyr327 (H5). Notably, BP-3 hydrophobically interacted with Tyr473, which is the major characteristic of PPARγ full agonism (Capelli et al., 2016). BP-8 formed at least three hydrogen bonds with Ser342 (β3). The 2-hydroxyl group of the phenyl moiety of BP-8 formed a hydrogen bond with the backbone amine nitrogen of Ser342. Another 2-hydroxyl group in the 4-methoxyphenyl moiety of BP-8 interacted with the backbone amine nitrogen and the hydroxyl oxygen of Ser342 as well. In addition, BP-8 hydrophobically interacted with Ile281 (H3), Gly284 (H3), and Arg288 (H3). The optimized binding mode of BP-8 to PPARγ-LBD suggested that BP-8 acts as a PPARγ partial agonist (Kroker and Bruning, 2015; Capelli et al., 2016).

The binding modes in the molecular modeling stimulation suggests that BP-3 functioned as a PPARγ full agonist whereas BP-8 was a partial agonist. Full agonists generally exhibit additive responses in competitive experiments. In contrast, partial agonists inhibit the

functional responses of full agonists because less potent partial agonists compete with the full agonist at the PPARγ binding site (Hoyer and Boddeke, 1993; Ahn et al., 2018). To experimentally confirm the binding mechanisms of BP-3 and BP-8, pioglitazone, a clinically prescribed PPARγ full agonist, was co-treated during adipogenesis in hBM-MSCs. When co-treated with pioglitazone, BP-3 exhibited additive responses to the concentration-dependent effect of pioglitazone on adiponectin promotion, indicating that BP-3 acted as a PPARγ full agonist. However, BP-8 antagonized the effect of pioglitazone on adiponectin production (Fig. 7D and E). These results confirmed that BP-3 functions as a PPARγ full agonist, whereas BP-8 act as a PPARγ partial agonist.

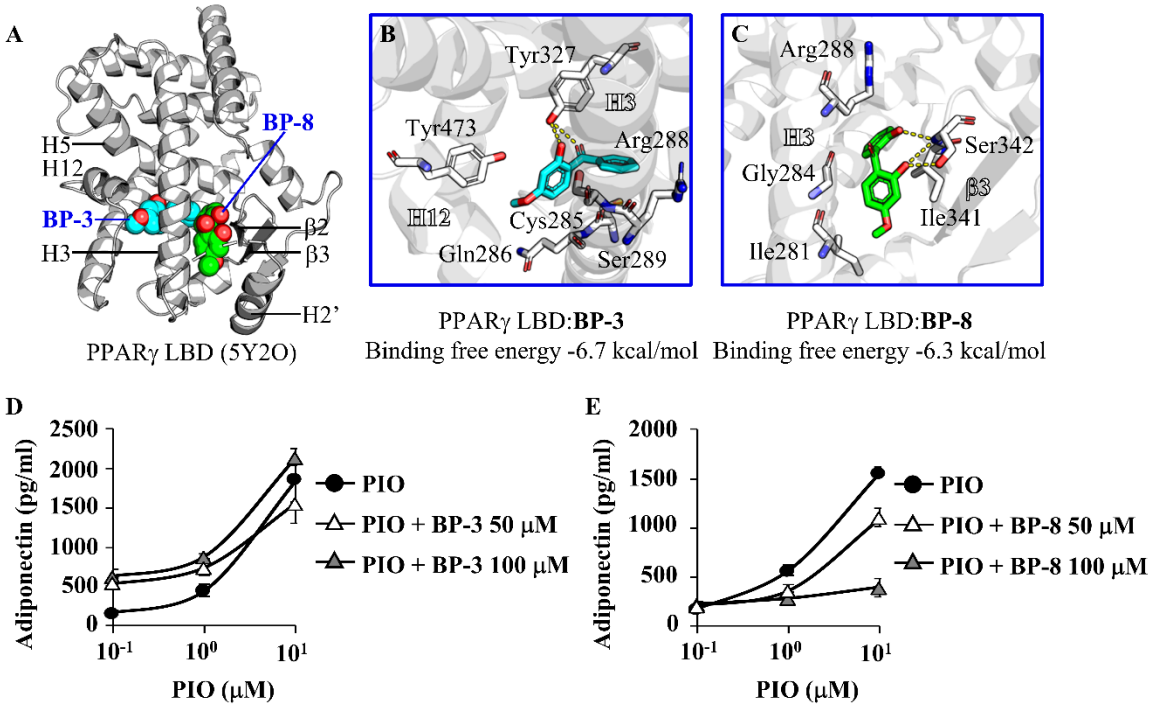

Figure 7. Binding modes of PPARγ ligand binding domain

(A) Binding models of BP-3 and BP-8 were simulated and overlaid in PPARγ-LBD. Secondary structures are shown as ribbons, and structure of BP-3 (cyan) and BP-8 (green) are presented as spheres. Docking simulation was conducted using AutoDock Vina software. H, helix; β, β-sheet. (B) BP-3 in ligand-binding pocket near H12. Helices are transparent for clarity. Residues in close contact to BP-3 were labeled. Oxygen and nitrogen atoms are colored in red and blue, respectively. Hydrogen bonds are presented as yellow dashes. (C) BP-8 in ligand-binding pocket near β-sheets. The closely contacting residues to BP-8 were labeled. Hydrogen bonds are presented as yellow dashes. All graphics were prepared using PyMOL software. Experimental validation of PPARγ-dependent mechanism of (D) BP-3 and (E) BP-8 was performed. hBM-MSCs were differentiated using IDX medium. BP-3 and BP-8 were co-treated with pioglitazone, a PPARγ full agonist.

3-4. BP-3 and BP-8 upregulated gene transcription of PPARα and PPARγ in normal human epidermal keratinocytes (NHEKs)

The primary target organ of sunscreen products is the human skin. Next, we investigated whether BP-3 and BP-8 directly affect the transcription of lipid metabolism-associated genes. To confirm whether BPs induce metabolic changes in human skin, mRNA levels of PPARα, PPARγ, HMGCR, HMGCS1, FASN and FADS1 were measured 24 h after treating NHEKs with BP-3 and BP-8 using Q-RT-PCR (Fig. 8). Avobenzone, used as a positive obesogenic sunscreen ingredient, increased the gene transcription of PPARα and PPARγ in NHEKs (Ahn et al., 2019). BP-3 and BP-8 concentration-dependently increased mRNA levels of PPARα and PPARγ compared to the control (Fig. 8A and B). Avobenzone also induced gene transcriptional changes in major enzymes regulating cholesterol metabolism such as HMGCR and HMGCS1 (Lee et al., 2018a; Ahn et al., 2019). The mRNA levels of HMGCR and HMGCS1 were significantly upregulated in NHEKs by BP-3 and BP-8 (Fig. 8C and D). These results showed that BP sunscreen ingredients BP-3 and BP-8 have direct metabolic effects on human skin. Therefore, BP-3 and BP-8 are potential human obesogens similar to avobenzone (Ahn et al., 2019).

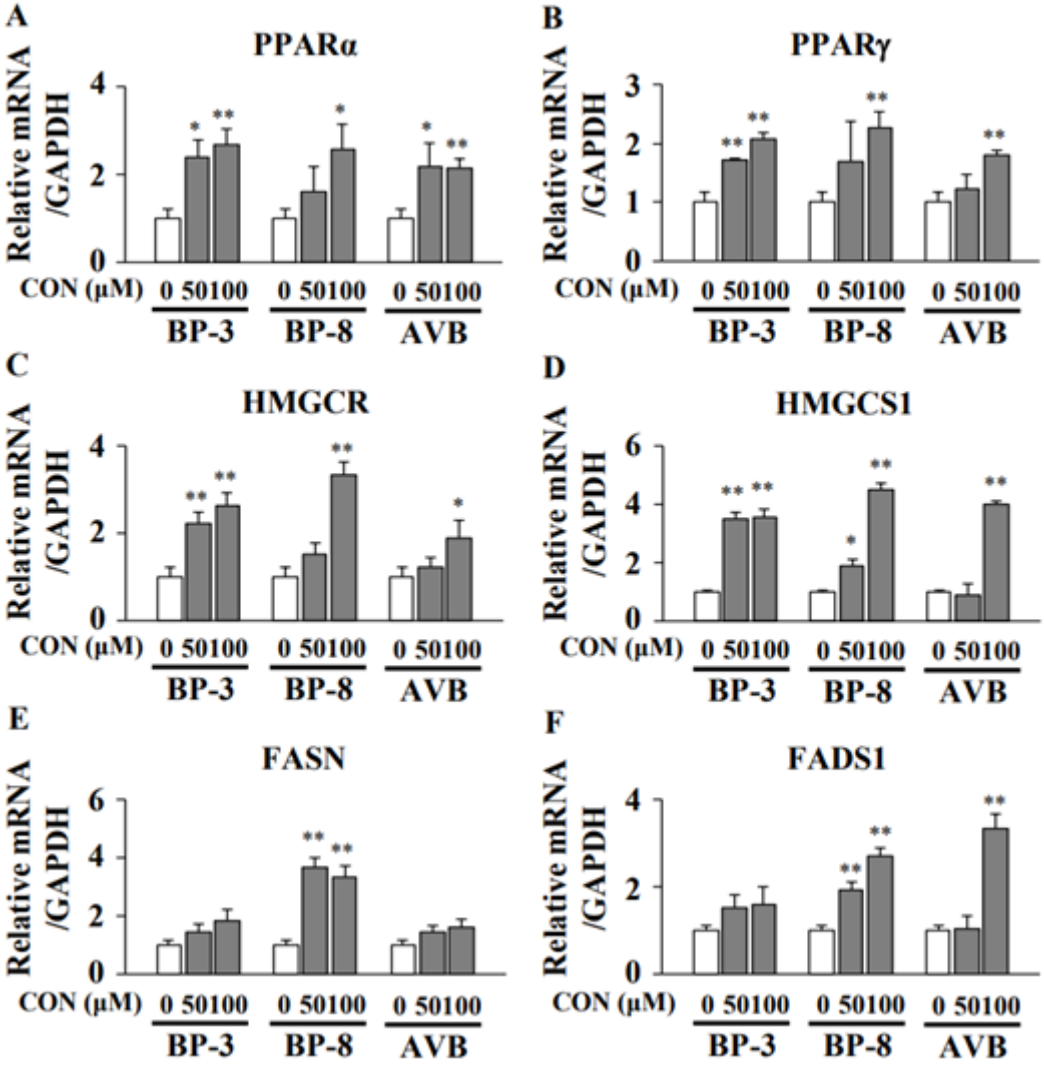

Figure 8. The effect of BP-3 and BP-8 on transcription of lipid metabolism-associated genes in NHEKs

Total RNA samples were extracted from confluently cultured NHEKs treated with BP-3, BP-8, and AVB for 24 h. The mRNA levels of PPARα (A), PPARγ (B), HMGCR (C), HMGCS1 (D), FASN (E), and FADS1 (F) were measured by Q-RT-PCR. Values represent the mean expression level ± SD (n=3) of the genes of interest relative to that of human GAPDH. *p < 0.05; ** p < 0.01.

4. Discussion

Chemical similarity has been used to predict potential toxic responses (McKinney et al., 2000). Recently, we reported the obesogenic activity of avobenzone. Among organic sunscreen ingredients approved in the EU and the US, BP-3 and BP-8 exhibited the highest chemical similarity scores as determined by the Jaccard indexes with reference to avobenzone. As expected, BP-3 and BP-8, which are commonly used UV filters in cosmetic products, significantly promoted adipogenesis of hBM-MSCs and modified lipid metabolism in human keratinocytes similar to avobenzone. Although avobenzone positively affected adipocyte differentiation, it did not directly bind to PPARγ. In contrast, both BP-3 and BP-8 directly interacted with PPARγ and increased its transactivation responses. BP-3 was previously reported to be detected in fresh water environments at 0.4 to 1 μg/L concentrations (Ramos et al., 2015). Although information on residual amounts of BP-8 in environments is limited, its residual level was estimated to be approximately 117 ng/L in sea water (Ramos et al., 2015). The environmental residual levels of BP-3 and BP-8 are reported to be relatively higher than that of avobenzone because avobenzone is chemically unstable in the environment (Ramos et al., 2015). Consequently, BP-3 and BP-8 may have a greater environmental impact than avobenzone not only because of their direct effects on PPARγ but also their environmental residual amounts.

PPARγ is a direct transcriptional regulator of human adipogenesis (Janesick and Blumberg, 2011; Lefterova et al., 2014). Currently, mono-(2-ethylhexyl) phthalate (MEHP) and TBT have been demonstrated to be direct PPARγ binding ligands (Muscogiuri et al., 2017; Ahn et al., 2019). BP-3 and BP-8 exhibited competitive PPARγ binding activity. This study demonstrated that BP-3 functioned as a PPARγ full agonist and that BP-8 acted as a PPARγ partial agonist. Ligand-activated PPARγ forms a heterodimer with retinoid X receptors (RXRs). For

transcriptional activity, RXR-PPAR heterodimers need to interact with diverse coactivator proteins such as SRC-2, RAP250, DRIP-1, RIP140, and PGC-1α (Viswakarma et al., 2010). Thiazolidinedione (TZD) class anti-diabetic drugs such as pioglitazone, a PPARγ full agonist, interact with virtually all coactivator proteins. In contrast, BP-3 and BP-8 binding to PPARγ only recruited SRC-2. SRC-2 knockout mice show obesity-resistant phenotypes such as increased energy consumption, decreased white adipocyte differentiation, and activated thermogenesis of brown adipocytes (Hartig et al., 2011). Consequently, BP-3- and BP8-induced recruitment of SRC-2 after their binding to PPARγ is the primary molecular mechanism of their obesogenic activity. Notably, the energy-minimized PPARγ-binding model suggests that BP-3 interacts with Tyr473 (H12) in PPARγ-LBD, which is the most essential feature of the X-ray crystal structure of PPARγ full agonist binding (Jang et al., 2019). The molecular model of the interaction between BP-8 and PPARγ exhibited the typical binding mode for PPARγ partial agonists, lacking the interaction with Tyr473. Arg288 (H3), the amino acid residue in helix H3 of PPARγ-LBD commonly interacting with both BP-3 and BP-8 in the PPARγ-binding models, may be associated with the recruitment of SRC-2 to RXR-PPARγ, which requires validation in future studies.

BPs in sunscreen products have great impact on human health because they are extensively used and exposed to the environment. The annual European industrial production of BP-3 is estimated at between 100 and 1000 tons and approximately 10 tons for BP-8 (ECHA, 2018a; ECHA, 2018b). The annual report of the US Center for Disease Control (CDC) on human exposure to environmental chemicals showed that BP3 was detected in urine samples from 97% of the people tested. Notably, BPs were significantly concentrated in fresh waters and aquatic organisms (Calafat et al., 2008). Especially, due to growing concerns regarding coral reefs and other marine ecosystems, the state government of Hawaii passed a bill that prohibits the sale and distribution of sunscreen products containing BP-3 (Schneider and Lim, 2019). Notably, a

significant level of BP-1 has been detected in environments (Calafat et al., 2008). Although BP-1 is not currently permitted to be used in sunscreen products, it is extensively used in nail polish products. BP-1, a well-known endocrine disrupting compound, has a stronger estrogenic activity than BP-3 (Kunz et al., 2006). In addition, elevated BP-1 levels have been suggested to be associated with diverse estrogen-dependent diseases (Kunisue et al., 2012). Considering the chemical similarity of obesogenic BPs, BP-1 also has obesogenic potential and the propensity to affect human health, although this has not yet been experimentally validated. Systematic studies are required to qualitatively and quantitatively elucidate the obesogenic potentials of environmentally detected BP metabolites such as BP-1.

Organic UV filters absorb and subsequently dissipate UV radiation energy, which can induce toxic responses in human skin. Chemical similarity calculated using the Jaccard distance has limitations because it does not represent all physicochemical properties of compounds. The Jaccard similarity index is derived by dividing the number of shared chemical fingerprints with the total number of chemical fingerprints of two compounds (Cereto-Massagué et al., 2015). In terms of physicochemical properties, other organic UV filters may have similar toxicities to those of BPs, which necessitates a systematic investigation of the potential effects of approved UV filters on adipogenesis in hBM-MSCs in future.

In conclusion, this study showed that BP-3 and BP-8 are environmental obesogens that act via a PPARγ-SRC-2 dependent pathway. These BP sunscreen ingredients promote lipid droplet accumulation and adiponectin production during adipogenesis in hBM-MSCs and change the gene transcriptional activity of essential lipid metabolizing enzymes in NHEKs. Furthermore, we demonstrated that BP-3 functions as a PPARγ full agonist whereas BP-8 acts as a partial agonist. This study highlights the effects of sunscreen ingredients as major environmental obesogens similar to phthalates, bisphenols, and organotins.

5. References

1. Ahn, S., Lee, M., An, S., Hyun, S., Hwang, J., Lee, J., Noh, M., 2018. 2-Formyl-komarovicine promotes adiponectin production in human mesenchymal stem cells through PPARγ partial agonism. Bioorg Med Chem 26, 1069-1075. https://doi.org/10.1016/j.bmc.2018.01.019.

2. Ahn, S., An, S., Lee, M., Lee, E., Pyo, J.J., Kim, J.H., K,i M.W., Jin, S.H., Ha, J., Noh, M., 2019. A long-wave UVA filter avobenzone induces obesogenic phenotypes in normal human epidermal keratinocytes and mesenchymal stem cells. Arch Toxicol 93, 1903-1915. https://doi.org/10.1007/s00204-019-02462-1.

3. Calafat, A.M., Wong, L.Y., Ye, X., Reidy, J.A., Needham, L.L., 2008. Concentrations of the sunscreen agent benzophenone-3 in residents of the United States: National Health and Nutrition Examination Survey 2003-2004. Environ Health Perspect 116, 893-897. https://doi.org/10.1289/ehp.11269.

4. Capelli, D., Cerchia, C., Montanari, R., Loiodice, F., Tortorella, P., Laghezza, A., Cervoni, L., Pochetti, G., Lavecchia, A., 2016. Structural basis for PPAR partial or full activation revealed by a novel ligand binding mode. Sci Rep 6, 34792. https://doi.org/10.1038/srep34792.

5. Cereto-Massagué, A., Ojeda, M. J., Valls, C., Mulero, M., Garcia-Vallvé, S., Pujadas, G., 2015. Molecular fingerprint similarity search in virtual screening. Methods 71, 58–63. https://doi.org/10.1016/j.ymeth.2014.08.005.

6. Collins, P., Ferguson, J., 1994. Photoallergic contact dermatitis to oxybenzone. Br J Dermatol 131, 124-129. https://doi.org/10.1111/j.1365-2133.1994.tb08469.x.

7. ECHA, 2018a. Registered substances CAS 131-57-7. https://www.echa.europa.eu/web/guest/registration-dossier/-/registered-dossier/5515. (accessed 9 Mar 2020).

8. ECHA, 2018b. Registered substances CAS 131-53-3. https://www.echa.europa.eu/web/guest/registration-dossier/-/registered-dossier/23375. (accessed 9 Mar 2020).

9. Ghazipura, M., McGowan, R., Arslan, A., Hossain, T., 2017. Exposure to benzophenone-3 and reproductive toxicity: A systematic review of human and animal studies. Reprod Toxicol 73, 175-183. https://doi.org/10.1016/j.reprotox.2017.08.015.

10. Han, M.H., Kim, H.J., Jeong, J.W., Park, C., Kim, B.W., Choi, Y.H., 2018. Inhibition of adipocyte diferentiation by anthocyanins isolated from the fruit of vitis coignetiae pulliat is associated with the activation of AMPK signaling pathway. Toxicol Res 34,13. https://doi.org/10.5487/TR.2018.34.1.013

11. Hartig, S.M., He, B., Long, W., Buehrer, B.M., Mancini, M.A., 2011. Homeostatic levels of SRC-2 and SRC-3 promote early human adipogenesis. J Cell Biol 192, 55-67. https://doi.org/10.1083/jcb.201004026.

12. Heindel, J.J., Blumberg, B., 2019. Environmental obesogens: mechanisms and controversies. Annu. Rev. Pharmacol. Toxicol. 59, 89–106. https://doi.org/10.1146/ annurev-pharmtox-010818-021304

13. Heurung, A.R., Raju, S.I., Warshaw, E.M., 2014. Adverse reactions to sunscreen agents: epidemiology, responsible irritants and allergens, clinical characteristics, and management. Dermatitis 25, 289-326. https://doi.org/10.1097/DER.0000000000000079.

14. Hoyer, D., Boddeke, H.W., 1993. Partial agonists, full agonists, antagonists: dilemmas of definition. Trends Pharmacol. Sci. 14, 270–275. https://doi.org/10.1016/0165- 6147(93)90129-8.

15. Janesick, A., Blumberg, B., 2011. Minireview: PPARγ as the target of obesogens. J Steroid Biochem Mol Biol 127, 4-8. https://doi.org/10.1016/j.jsbmb.2011.01.005.

16. Jang, J.Y., Kim, H., Kim, H.J., Suh, S.W., Park, S.B., Han, B.W., 2019. Publisher Correction: Structural basis for the inhibitory effects of a novel reversible covalent ligand on PPARγ phosphorylation. Sci Rep 9, 15798. https://doi.org/10.1038/s41598-019-50831-8.

17. Jansen, R., Osterwalder, U., Wang, S.Q., Burnett, M., Lim, H.W., 2013. Photoprotection: part II. Sunscreen: development, efficacy, and controversies. J Am Acad Dermatol 69, 867e1-e14. https://doi.org/10.1016/j.jaad.2013.08.022.

18. Kroker, A.J., Bruning, J.B., 2015. Review of the Structural and Dynamic Mechanisms of PPARγ Partial Agonism. PPAR Res 2015, 816856. https://doi.org/10.1155/2015/816856.

19. Kunisue, T., Chen, Z., Buck Louis, G.M., Sundaram, R., Hediger, M.L., Sun, L., Kannan, K., 2012. Urinary concentrations of benzophenone-type UV filters in U.S. women and their association with endometriosis. Environ Sci Technol 46, 4624-4632. https://doi.org/10.1021/es204415a.

20. Kunz, P.Y., Galicia, H.F., Fent, K., 2006. Comparison of in vitro and in vivo estrogenic activity of UV filters in fish. Toxicol Sci 90, 349-361. https://doi.org/10.1093/toxsci/kfj082.

21. Lee, M.A., Tan, L., Yang, H., Im, Y.G., Im, Y.J. 2017. Structures of PPARγ complexed with lobeglitazone and pioglitazone reveal key determinants for the recognition of antidiabetic drugs. Sci Rep 7, 16837. https://doi.org/10.1038/s41598-017-17082-x.

22. Lee, H., Cheong, K.A., Kim, J.Y., Kim, N.H., Noh, M., Lee, A.Y., 2018a. IL-1 Receptor Antagonist Reduced Chemical-Induced Keratinocyte Apoptosis through Antagonism to IL-1α/IL-1β. Biomol Ther 26, 417-423. https://doi.org/10.4062/biomolther.2017.167.

23. Lee, J., Kim, S., Park, Y. J., Moon, H. B., Choi, K., 2018b. Thyroid hormone-disrupting potentials of major benzophenones in two cell lines (GH3 and FRTL-5) and embryo-larval zebrafish. Environ Sci Technol 52, 8858-8865. https://doi.org/10.1021/acs.est.8b01796.

24. Lefterova, M.I., Haakonsson, A.K., Lazar, M.A., Mandrup, S., 2014. PPARγ and the global map of adipogenesis and beyond. Trends Endocrinol Metab 25, 293-302. https://doi.org/10.1016/j.tem.2014.04.001.

25. Luechtefeld, T., Marsh, D., Rowlands, C., Hartung, T., 2018. Machine learning of toxicological big data enables read-across structure activity relationships (RASAR) outperforming animal test reproducibility. Toxicol. Sci. 165, 198–212. https://doi.org/ 10.1093/toxsci/kfy152

26. Ma, X., Wang, D., Zhao, W., Xu, L., 2018. Deciphering the Roles of PPARγ in Adipocytes via Dynamic Change of Transcription Complex. Front Endocrinol (Lausanne) 9, 473. https://doi.org/10.3389/fendo.2018.00473.

27. Mao, F., You, L., Reinhard, M., He, Y., Gin, K.Y., 2018. Occurrence and Fate of Benzophenone-Type UV Filters in a Tropical Urban Watershed. Environ Sci Technol 52, 3960-3967. https://doi.org/10.1021/acs.est.7b05634.

28. McKinney, J.D., Richard, A., Waller, C., Newman, M.C., Gerberick, F., 2000. The practice of structure activity relationships (SAR) in toxicology. Toxicol Sci 56, 8-17. https://doi.org/10.1093/toxsci/56.1.8.

29. Muscogiuri, G., Barrea, L., Laudisio, D., Savastano, S., Colao, A., 2017. Obesogenic endocrine disruptors and obesity: myths and truths. Arch Toxicol 91, 3469-3475. https://doi.org/10.1007/s00204-017-2071-1.

30. Pfaffl, M.W., 2001. A new mathematical model for relative quantification in real-time RT–PCR. Nucleic Acids Res 29, e45. https://doi.org/10.1093/nar/29.9.e45.

31. Ramos, S., Homem, V., Alves, A., Santos, L., 2015. Advances in analytical methods and occurrence of organic UV-filters in the environment-A review. Sci Total Environ 526, 278-311. https://doi.org/10.1016/j.scitotenv.2015.04.055.

32. Schneider, S.L., Lim, H.W., 2019. Review of environmental effects of oxybenzone and other sunscreen active ingredients. J Am Acad Dermatol 80, 266-271. https://doi.org/10.1016/j.jaad.2018.06.033.

33. Trott, O., Olson, A.J., 2010. AutoDock Vina: improving the speed and accuracy of docking with a new scoring function, efficient optimization and multithreading. J Comput Chem 31, 455−461. https://doi.org/10.1002/jcc.21334.

34. Viswakarma, N., Jia, Y., Bai, L., Vluggens, A., Borensztajn, J., Xu, J., Reddy, J.K., 2010. Coactivators in PPAR-Regulated Gene Expression. PPAR Res 2010, 250126. https://doi/org/10.1155/2010/250126.

35. Wallace, A.C., Laskowski, R.A., Thornton, J.M., 1995. LIGPLOT: a program to generate schematic diagrams of protein-ligand interactions. Protein Eng 8, 127-134. https://doi.org/10.1093/protein/8.2.127.

36. Wang, S.Q., Lim, H.W., 2011. Current status of the sunscreen regulation in the United States: 2011 Food and Drug Administration's final rule on labeling and effectiveness testing. J Am

Acad Dermatol 65, 863-869. https://doi.org/10.1016/j.jaad.2011.07.025.

요약 (국문초록)

벤조페논 계열 자외선차단체의

PPARγ 기전을 통한 비만유도 활성 연구

신 지 영

서울대학교 대학원

약학과 천연물과학전공

벤조페논-3(BP-3)와 벤조페논-8(BP-8)은 다양한 자외선 차단 제품에서 흔히 사용되는 자외선 (UV) 필터 성분이다. 최근 UV A 필터인 아보벤존의 비만유도 활성이 인간 골수유래 중간엽줄기세포(hBM-MSC)의 지방 생성 모델에서 밝혀졌다. 따라서 아보벤존과 화학구조적 유사성을 보이는 BP-3와 BP-8의 비만유도 가능성을 연구하였다. hBM-MSC의 지방분화 과정에서 BP-3와 BP-8 (각각 EC_{50}, 25.05 와 43.20 μM)은 아보벤존 (EC_{50}, 72.69 μM)보다 더 강력하게 아디포넥틴 분비를 촉진시킨다는 것을 확인하였다. 표적규명 연구에서 BP-3와 BP-8 모두 페록시솜 증식체 활성화수용체 γ (PPARγ)에 직접 결합함을 확인하였으며, 이들의 PPARγ 결합은 스테로이드 수용체 보조 활성화제-2 (SRC-2)의 활성화로 이어질 수 있었다. 이는 관찰된 비만유도 활성이 PPARγ 의존 경로를 통해 나타난다는 사실을 뒷받침한다. BP-3와 BP-8은 각각 PPARγ 완전 및 부분 작용제로 기능하였다. 또한 벤조페논은 사람 피부에서 UV 필터의 주요 표적 부위인 표피 각질 세포에서 PPARα, PPARγ, 및 주요 지질 대사 관련 효소의 유전자 전사를 크게 증가시켰다. 따라서, 본 연구는 BP-3와 BP-8이 프탈레이트,

비스페놀 및 유기주석 화합물과 같이 비만유도 화학물질로 작용할 수 있음을 시사한다.

주요어: 벤조페논-3, 벤조페논-8, PPARγ, 인간 골수유래 중간엽줄기세포, 비만유도

학번: 2018-21004